Journal of Hydroscience and Hydraulic Engineering
Vol. 5, No. 1, July, 1987, pp.11-26.

SEDIMENT TRANSPORT IN STEEP CHANNELS

By

Walter H. Graf and Lechoslaw Suszka
Laboratoire d'hydraulique, Ecole Polytechnique Fédérale, Lausanne, Switzerland

SYNOPSIS

Sediment transport in relatively steep channels, mainly in form of bed load, is experimentally investigated. An accurately performing sediment-measuring device was developed. The obtained data are presented in dimensionless form and compared with other existing data sets. A relation is proposed which does explain all of these data.

INTRODUCTION

Research at the Hydraulics Laboratory (LHYDREP) of the Ecole Polytechnique Fédérale in Lausanne presently focuses on the understanding of the effects of unsteady flow on the sediment transport. Preliminary experiments have given rather interesting results; see Graf and Suszka (1985). However, before investigating the unsteady flow in detail, we must know rather well the steady flow and its effect on sediment transport. Herewith we communicate our present results on the sediment transport in form of bed load, at steady, uniform flow for relatively steep slopes within a range of $0.005 < S_0 < 0.025$.

First, the experimental setup and procedure is described. An accurately working sediment-measuring device (fig. 2) was developed, allowing continuous measurement of the sediment transport. Subsequently, the data will be presented in dimensionless form (fig. 4) and compared with other data found in the literature. A relation given with eq. 3 explains all the data reasonably well.

EXPERIMENTAL SETUP AND PROCEDURE

All experiments, were carried out in the Hydraulics Laboratory of the Ecole Polytechnique Fédérale de Lausanne during the period of 07.1984 to 10.1985. An already existing flume, which was constructed by Armfield Technical Education Co. Ltd. in 1979, was modified and adapted for our purpose; it is described in detail by Cao (1985).

Water circuit (fig. 1): It is a closed system in which water is recirculated. Water being drawn by two pumps from two sumps, flows through the operating valve continuing through the return pipe and electromagnetic flowmeter and reaches the headbox of the flume. After passing a combination of the grid and straightening tubes it flows through the flume to drop at the end into the collection tank which leads it back into the sump or into the pumping system.

The flume itself is 16.8 m long, 0.6 m wide and 0.8 m high, it has glass walls and a smooth steel floor to be covered with sediment. The flume is supported on a pivot at the drownstream part and by two pairs of columns of adjustable height at the centre and upstream end. It can be tilted about the pivot to slopes of - 1 % to 9.7 %. The floor of the flume can be modified for different purposes as was done for this work. Detaïled information about the actual state of the floor is given later.

Sediment circuit (fig. 1): During all experiments the sediment was supplied by eye-observation from the sediment hopper into the bed at a suitable rate to avoid a local erosion at the upstream part of the movable bed (nevertheless a test experiment showed that a sediment feeding during a single run is not perti-

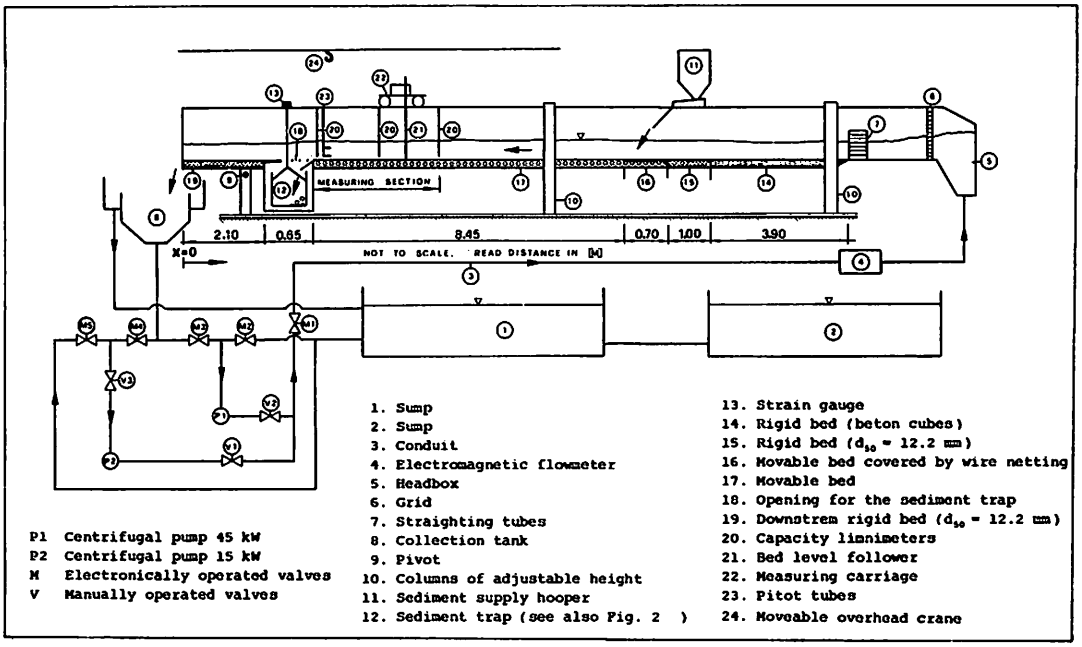

Fig. 1 Experimental Installation

nently necessary). After passing the measuring section, the sediment fell through a hole in the floor into the basket of the sediment trap.. The sediment, which accumulated in the basket was weighted continuously by a strain gauge. When the basket was almost full, it was removed with an overhead crane and emptied into a separate container. Such sediment was left for a certain period to dry and subsequently was transported into the silo of the sediment hopper. This recirculating procedure was repeated during each run.

The orginal steel floor of the flume was modified for our experiments; its new configuration is presented herewith. Starting from the upstream end of the flume the following sections of the bed are to be distinguished (the x-values represents distances relative to a zero point situated at the downstream end of the flume): (a) a rigid concrete bed with a length of 3.90 m is longer than is necessary to develop a turbulent boundary layer of a thickness δ equal to the flow depth h. In order to obtain uniform flow as fast as possible, small concrete cubes (40 x 30 x 20 mm) were fixed on a concrete bed. This concrete bed was installed into the flume (x = 12.90 to 16.80 m); (b) a rigid bed of 1 m length consisting of a single layer of the sediment glued to a PVC false floor in form of a box (1.00 x 0.60 x 0.08 m) was fixed directly onto the steel floor; (c) the first 0.7 m of the movable bed was additionally covered by a wire mesh to decrease the possibility of a local erosion (x = 11.20 to 11.90 m). The sediment used was d_{50} = 12.2 mm; (d) the movable bed including the measuring section was made up of a layer of loosly packed sediment to be investigated (d_{50} = 12.2 mm or d_{50} = 23.5 mm). The thickness of this layer was about 10 cm from the steel floor (x = 2.75 to 11.20 m); (e) the opening for the sediment trap (x = 2.10 to 2.75 m); (f) a rigid bed consisting of a single layer of sediment glued to PVC false bottom (as in a section (b)). This part of the bed was used to avoid an influence of possible backwater effects created by the downstream free overflow on the sediment trap and the measuring section.

To maintain an equilibrium state of the mobile bed, a sediment hopper was installed. It is composed of a storage silo and a vibrating sediment feeder manipulated manually by observation of the sediment bed. Sediment stored in the silo falls into a tilted gutter which is vibrated mechanically at a constant frequency. The sediment supply rate is proportional to the amplitude of the vibrations which can be adjusted by a potentiometer.

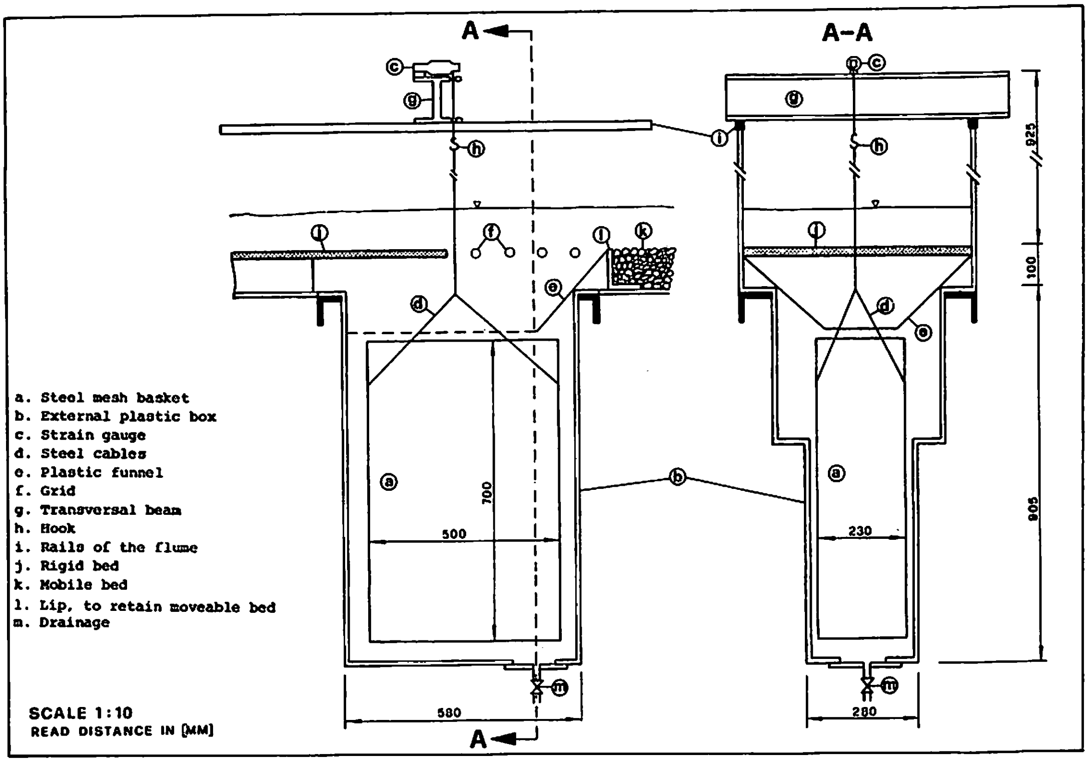

Fig. 2 Sediment Measuring Device (see also Photo 1)

A continuously accumulative sediment-measuring device (fig. 2) was designed, constructed and installed at the drownstream end of the measuring section. It consists of a basket [a], and external plastic box [b], and a strain gauge i.e.: a force (weight)-transducer [c]. The location of this installation and the dimensions of the trap were dictated by structural constraints imposed by the flume itself. A rectangular hole was cut in the flume's floor and a plastic box [b] (905 x 580 x 280 mm) was fixed under the floor to close this opening. The removable steel-mesh basket [a] (700 x 500 x 230 mm) was placed into this plastic box. It was suspended by 4 steel cables [d] of 6 mm diameter, linked to a force transducer. A plastic funnel [e] was installed to guide the sediment into the central section of the basket. On top of the opening, plastic tubes (filled with the sand) were placed in transversel direction to form a grid [f]. Spacing for the grid members was determined by trial and error to assure the uniformity of the water flow at this part of the flume. The strain gauge [c] was mounted on a transversel beam [g] which itself rests on the rails [i] of the flume at a height of 0.8 m above the floor of the flume. At the upper part of the basket the 4 cables were fixed to the force transducer to measure continuously the accumulative submerged weight of the sediment, accumulating in the basket. As a force transducer a type Z 6H2, produced by Hottinger-Baldwin Messtechnik, with a nominal maximum load value of 200 kG having a precision of 0.03 %, was chosen. When, after several runs the basket [a] was almost full, a hook [h] allowed to uncouple the transducer-cable-basket system. The laboratory's overhead crane was used to lift the basket which after emptying was reinstalled.

Some preliminary tests were carried out to check the sediment measuring device, which showed that: (i) the relation between the submerged weight of the empty basket plus sediment and the output voltage was linear but it contained considerable high frequency noise (to eliminate this, the signal was passed through a high-pass filter at the output by a calibration procedure relating weight (force), P [kG], to voltage output, U [volt], from the strain gauge); (ii) neither vibration of the water flow in the flume nor the sediment impacts

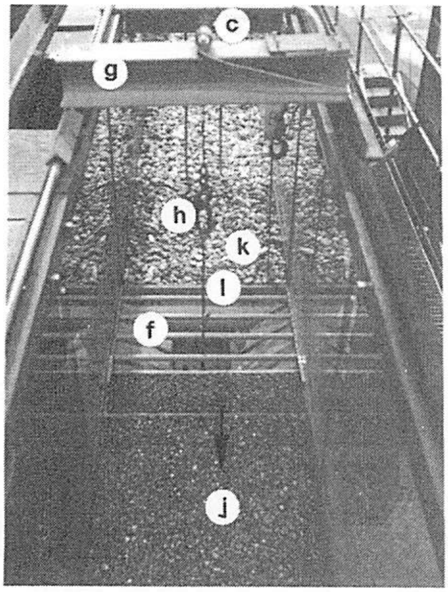

Longitudinal view

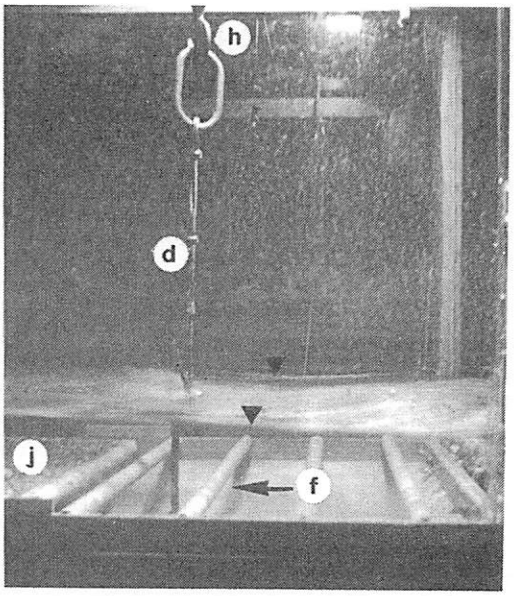

Side view

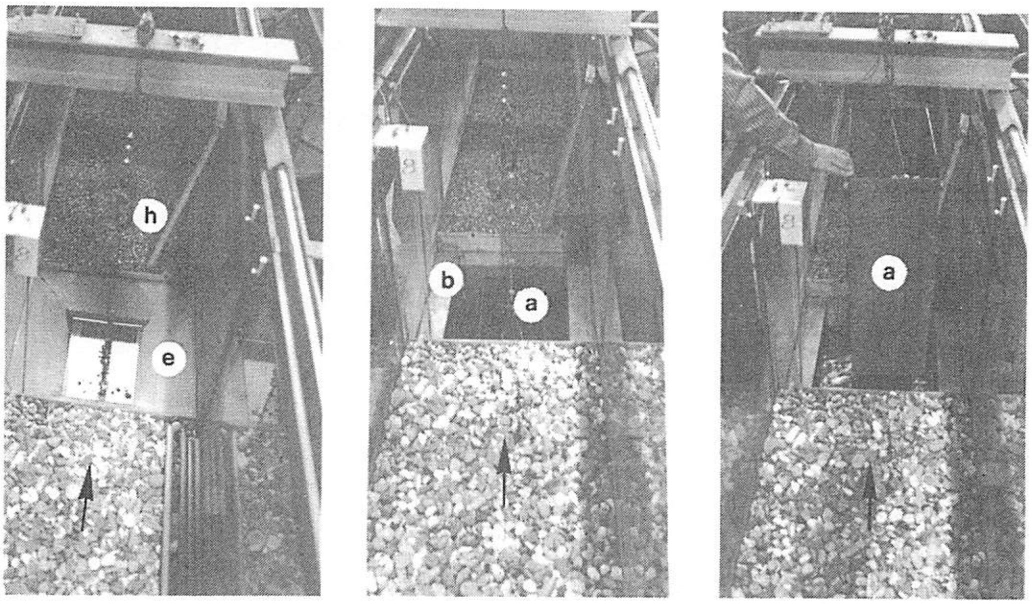

Emptying procedure

Photo 1 Sediment-measuring device
(for legend of symbols see fig. 2)

on the floor of the mesh basket did affect the stability of the recordings; (iii) in general no sediment overpassed the opening of the sediment trap; in rare exceptions, 2-5 particles were carried by the flow over the sediment trap; since this is a small quantity it was ignored; (iv) the maximum available volume of the sediment in the basket was 0.047 m^3.

The two sediments used in the experiments were each composed of commercially available (lake) gravel with relatively uniform size distributions. Their characteristics are summarized in Table 1. Size distributions were obtained by two methods, namely by sieving, with frequency analysis by weight and by surface sampling with frequency analysis by number. The specific gravity, γ_S, was determined for both the sediment particles and the bulk or packed material (particles plus voids). The angle of repose, Φ, was determined for the dried sediment simply by measuring the slope at which the sediment, if piled into a heap, became unstable.

Table 1 Summary of sediment characteristics

Sediments	Size distribution of median axis (mm) by								Specific gravity γ_s (g/cm³)		Porosity	Angle of repose Φ (degrees)	Krumbein intercept sphericity Ψ
	Sieving				Surface sampling				Particles only	(particles +voids)			
	d_{84}	d_{50}	d_{16}	σ	d_{84}	d_{50}	d_{16}	σ					
I	15.0	12.4	9.8	0.083	14.6	12.2	9.6	0.078	2.716	1.643	0.395	35.0	0.620
II	29.0	24.1	19.2	0.080	30.2	23.5	19.7	0.109	2.736	1.634	0.403	40.5	0.652

Note: d_n - size of median axis > n% of material in sample
σ - standard deviation = $\log(d_{84}/d_{50})$,
Ψ - $\sqrt[3]{d_{50}\, s_{50} / l_{50}^2}$, where l_{50} and s_{50} refer to long and short axis

Measuring devices (fig. 1): Three capacity limnimeters were made to measure the water levels as a function of time at three specific locations. A limnimeter consisted of two stainless steel wires 540 mm long with a diameter of 1.25 mm and spaced 10 mm apart. They are well stretched and are parallel in a frame constructed of 6 mm stainless steel rod; they are electrically insulated from the frame and from each other. The limnimeters were glued to the flume walls at a distance of 0.1 m. The first limnimeter was located slightly above the lip of the sediment trap at x = 2.83 m; the other ones were installed at the sections X = 4.03 m and x = 5.23 m, respectively. They were calibrated regularly before each experimental series in steady flow conditions, by means of point gauges installed during the calibration procedure at the neighbourhood of the limnimeters. A noticeable lack of the precision was due to the meniscus formed around the wires due to impurities; to decrease this error the wires had to be cleaned before each run with perchloroethylene.

An electronic profile indicator, PV-07, manufactured by the Delft Hydraulics Laboratory of Delft, NL, was used to measure the mean bed levels in two cross-sections before and after each run. The instrument consists of a 93 cm long probe pertruding vertically from its measuring unit. A servo-mechanism maintains the tip of the probe at a constant distance (0.5 - 2.5 mm) above the bed. If the instrument is displaced the probe follows continuously the configuration of the bed. The principle of the instrument is due to the appreciable difference between the electric conductivities of the water and the bed material. This profile indicator is mounted on the measuring carriage and can be displaced in longitudinal and transversal direction. In the experiments the profile indicator was employed at two control cross-sections, x = 4.03 m and x = 5.23 m, where the water levels were also recorded. Measurements of the bed levels could not be made in the near side wall regions; at left side of the flume (0.15 m) the probe of the bed-level follower was blocked by the capacity limnimeter, which was glued to the glass wall at the distance of 0.10 m, and at the right side (0.05 m), the flume was also inaccessible with respect of the dimensions of the bed-level follower. Thus only a central section of y = 0.40 m could be measured. The electric signal from the instrument was transmitted to a data acquisition system. The performance of the device is quite good, but problems arise if the probe encounters very rapid variation on the bed. In such a case the probe may get blocked and the output signal is faulty; the blocking particle had to be pushed slightly aside and the measurement was repeated right from the begining. Sensitivity of the instrument to bed variation, according to the producer, is 0.2 mm with a resolution 0.03 %.

Data acquisition system: A special system capable to obtain data with a high sampling rate called Front End (FE) was developed by the laboratory. The Front End (FE) acquires data only from a single experimental run. It records and stores the converted output voltages which arrive in parallel from the measuring devices with the same frequency and quantity. They measure hydraulic and sediment transport quantities, namely the three water levels, the bed level, the water discharge and the weight of sediment in the basket of the sediment-measuring device; these are related by an adequate proportionality factor. From the three limnimeters and the electromagnetic flowmeter the output voltage comes directly into FE. The same is obtained with the strain gauge, which converts the weight of the (filled) basket with the sediment to a voltage. The FE digitizes the information obtained as the output voltages. After each experimental run, the digitized information is transmitted in the form of a data file from the FE into a computer, in our case a VAX 780. The new data files are stored on the computer disc and recorded on the magnetic band. The pre-established programmes convert the data from digitized to the analoge format. The data can be treated subsequently on a base of the relations obtained earlier from the calibrations of the devices to get the real values of the parameters mesured.

Experimental procedure: Before commencement of a series of experiments a number of operations were necessary: (i) the storage silo and the basket of the sediment measuring device were checked and then filled or emptied if necessary; (ii) the electric wires of the limnimeters were carefully cleaned with the perchloroethylene; (iii) a flow exceeding slightly the beginning of sediment transport was introduced into the flume for a short period, in order to arrange "naturally" the sedimentary bed. This was particularly important for the small discharge experiments, since this flow was too weak to adjust naturally the sedimentary bed; (iv) then, the water discharge was decreased, and the bed-level follower was used for the bed-level measurements at two sections of the moveable bed i.e. at x = 5.23 m and 4.03 m respectively. The output signal from the bed-level follower, which was proportional to the bed level was recorded on the data acquisition system (FE) with the frequency of 1 Hz.

The steady flow experiments could be performed. (i) Point gauges were installed close to each of the three limnimeters to allow for calibration of these in flowing water conditions. (ii) The limited volume of the basket of the sediment measuring device requires for two input parameters to be introduced into the FE. The first parameter indicates a frequency between the sampling of the data by the FE; and the second one specifies the number of values which have to be recorded. The range of frequencies used was between 0.2 and 2 Hz, for the maximum and minimum discharge, respectively. The range of water discharges used during experiments was imposed not only by the limited volume of the basket, but also by the range of the water discharges to be used later in the unsteady flow experiments. (iii) When the required water discharge was fixed i.e.: uniform flow conditions were attained in the flume, the FE started the recording procedure. (iv) During the experiment the water levels at the measuring cross-sections were measured manually with the point gauges. Five to ten readings were taken, averaged and subsequently compared with the mean output signal from the limnimeters recorded on the FE. (v) If sediment transport occurred, the sediment supply from the sediment hopper at the upstream end of the movable bed was controled manually (thus another person was necessary during this phase of the experiments). (vi) The basket of the sediment-measuring system was recorded on the FE. Simultaneously the water discharge from the flowmeter was recorded on the FE. (vii) The discharge was then decreased below the critical one. (ix) All data were transmitted from the FE into the disc of the VAX computer and later stored on the magnetic band, thus the FE was free for data from the next cross-sections measurements. (x) The procedure of the measurement of the bed cross-sections by the bed follower (profiler) was repeated after each run in the same manner as at the beginning of the run. On the base of the average bed levels at cross-sections measured before and after the run, the behaviour of the bed during the experiment was estimated by simple interpolation. (xi) At the end of each experiment, the water temperature was measured manually and the kinematic viscosity could be determined. (xii) A new experiment could be started, but if the pumps were turned off, the same preparation procedure had to be repeated to obtain suitable conditions for the next experiment.

At steady flow conditions a total of 114 experiments (see Table 2) were carried out; sediment transport occurred in 106 cases, while in 8 experiments the flow was too weak to produce a measurable sediment transport.

PRESENTATION OF DATA

All experiments were performed under equilibrium conditions i.e.: (i) when the sediment supplied was approximately equal to sediment collected by the sediment-measuring device and this during the entire period of the experiment; (ii) when the mean bed level in the measuring section did not change considerably ($\Delta z < 0.3$ cm).

Two sediments (Table 1) were chosen as a bed material; for sediment I (d_{50} = 12.2 mm) 80 and for sediment II (d_{50} = 23.5 mm) 34 experiments were carried out for different slopes and for different water discharges. The data obtained are tabulated in Tables 2a and 2b; the legend of these tables is largely selfexplanatory; it shall suffice to make only a few remarks. The water stages were measured by point gauges at three different measuring cross-sections; at the same sections the bed levels were measured before and after each experiment by the bed-level follower. The water depths were determined as the difference between the water stage and the bed level measured at the same measuring sections. For further calculations the average water depth, h, from these three measuring sections was used; it served also, after correction for wall effects, to calculate the hydraulic radius, R_h (see Suszka (1986, App. B)). The water discharge, Q, was obtained with an electromagnetic flowmeter and the sediment discharge (volume of particles only), Qs_0, was determined with sediment-measuring device installed downstream of the measuring cross-sections. Time duration of each experiment was dictated by the limited volume of the basket of the sediment-measuring device; it ranged from 240 sec for strong sediment transport to 3600 sec for weak transport. Due to the possibility of continuously recording the sediment discharges the fluctuations of these during steady, uniform flow were noticed to be considerable. Their presentation and interpretation is found in Suszka (1986). During all experiments the prevailing mode of sediment transport was as bed load. Furthermore only a "plane bed" was observed; this is due to high Froude-number flow ($Fr > 0.8$) as well as accurate supply of sediment at the upstream part of the movable bed.

The data are graphically displayed on the figs. 3a and 3b. For a given water depth, h, and water discharge, Q, the sediment discharge, Qs_0, can be obtained; the slope, S_0, being the parameter.

DIMENSIONLESS PRESENTATION OF DATA

For verification of the consistency of the present data they ought to be plotted in dimensionless form and compared with other data as well as with "theoretical" relationships which are available in the literature.

Sediment transport: Because certain parameters (most prominently the splitting up of the hydraulic radius, as $R_h = R_h' + R_h''$) used in different sediment transport relations, cannot be readily evaluated, the calculations proceed herewith according to the parameters of the Graf and Acaroglu (1968) approach (see Graf (1971, p. 218)), where the shear-intensity parameter,

Table 2a Summary of data (steady, uniform flow); sediment I

No	d_{50} [m]	S_o	h [m]	R_h [m]	Q [m³/s]	Qs_o [m³/s]	ν [m²/s]	U [m/s]	U_* [m/s]	U/U_*	h/d50	τ [N/m²]	τ_*	Re_*	Ψ	Φ	qs_o [m²/sm]
101	0.0122	0.0075	0.084	0.078	0.039	0.000E+00	0.107E-05	0.774	0.076	10.187	6.89	5.8	0.0282	868.	35.47	0.000E+00	0.000E+00
102	0.0122	0.0075	0.093	0.087	0.044	0.000E+00	0.105E-05	0.789	0.080	9.876	7.62	6.4	0.0312	929.	32.10	0.000E+00	0.000E+00
103	0.0122	0.0075	0.118	0.108	0.065	0.477E-07	0.102E-05	0.918	0.089	10.303	9.67	7.9	0.0388	1061.	25.78	0.132E-04	0.795E-07
104	0.0122	0.0075	0.124	0.113	0.071	0.127E-06	0.102E-05	0.954	0.091	10.478	10.16	8.3	0.0405	1087.	24.67	0.349E-04	0.212E-06
105	0.0122	0.0075	0.132	0.119	0.078	0.147E-06	0.101E-05	0.985	0.094	10.505	10.82	8.8	0.0429	1134.	23.29	0.402E-04	0.245E-06
106	0.0122	0.0075	0.139	0.125	0.085	0.786E-06	0.997E-06	1.019	0.096	10.623	11.39	9.2	0.0450	1174.	22.24	0.214E-03	0.131E-05
107	0.0122	0.0075	0.147	0.132	0.093	0.158E-05	0.982E-06	1.054	0.098	10.714	12.05	9.7	0.0473	1223.	21.13	0.427E-03	0.263E-05
108	0.0122	0.0075	0.155	0.138	0.102	0.277E-05	0.997E-06	1.097	0.101	10.893	12.70	10.1	0.0495	1232.	20.19	0.744E-03	0.462E-05
109	0.0122	0.0075	0.161	0.143	0.106	0.407E-05	0.992E-06	1.097	0.103	10.694	13.20	10.5	0.0514	1262.	19.44	0.109E-02	0.678E-05
110	0.0122		0.162	0.143	0.109	0.509E-05	0.967E-06	1.121	0.103	10.916	13.28	10.6	0.0516	1296.	19.39	0.136E-02	0.848E-05
111	0.0122	⊗	0.169	0.149	0.117	0.779E-05	0.972E-06	1.154	0.105	11.030	13.85	10.9	0.0535	1313.	18.70	0.207E-02	0.130E-04
112	0.0122		0.174	0.152	0.124	0.974E-05	0.964E-06	1.188	0.106	11.220	14.26	11.2	0.0548	1340.	18.26	0.257E-02	0.162E-04
113	0.0122		0.182	0.159	0.131	0.114E-04	0.931E-06	1.200	0.108	11.091	14.92	11.7	0.0572	1417.	17.49	0.301E-02	0.190E-04
114	0.0122	0.0075	0.192	0.167	0.141	0.186E-04	0.104E-05	1.224	0.111	11.055	15.74	12.3	0.0599	1293.	16.70	0.487E-02	0.310E-04
115	0.0122	0.0075	0.201	0.173	0.152	0.271E-04	0.103E-05	1.260	0.113	11.166	16.48	12.7	0.0622	1337.	16.06	0.705E-02	0.452E-04
116	0.0122	0.0075	0.209	0.180	0.160	0.336E-04	0.103E-05	1.276	0.115	11.102	17.13	13.2	0.0645	1365.	15.49	0.872E-02	0.560E-04
117	0.0122	0.0075	0.217	0.185	0.170	0.393E-04	0.102E-05	1.306	0.117	11.180	17.79	13.6	0.0666	1401.	15.01	0.101E-01	0.655E-04
118	0.0122	0.0075	0.229	0.194	0.185	0.534E-04	0.106E-05	1.346	0.119	11.278	18.77	14.3	0.0696	1373.	14.36	0.136E-01	0.890E-04
119	0.0122	0.0075	0.236	0.198	0.196	0.618E-04	0.103E-05	1.384	0.121	11.458	19.34	14.6	0.0713	1435.	14.02	0.157E-01	0.103E-03
201	0.0122	0.0050	0.133	0.118	0.070	0.000E+00	0.104E-05	0.877	0.076	11.528	10.90	5.8	0.0283	893.	35.35	0.000E+00	0.000E+00
202	0.0122	0.0050	0.142	0.125	0.079	0.000E+00	0.102E-05	0.927	0.078	11.857	11.64	6.1	0.0299	936.	33.46	0.000E+00	0.000E+00
203	0.0122	0.0050	0.154	0.134	0.090	0.000E+00	0.102E-05	0.974	0.081	12.025	12.62	6.6	0.0321	964.	31.19	0.000E+00	0.000E+00
204	0.0122	0.0050	0.163	0.140	0.099	0.187E-06	0.101E-05	1.012	0.083	12.203	13.36	6.9	0.0336	998.	29.74	0.486E-04	0.312E-06
205	0.0122	0.0050	0.175	0.150	0.109	0.349E-06	0.100E-05	1.038	0.086	12.109	14.34	7.4	0.0359	1042.	27.84	0.902E-04	0.582E-06
206	0.0122	0.0050	0.185	0.157	0.118	0.653E-06	0.100E-05	1.063	0.088	12.103	15.16	7.7	0.0377	1072.	26.53	0.168E-03	0.109E-05
207	0.0122	0.0050	0.195	0.164	0.129	0.115E-05	0.989E-06	1.103	0.090	12.286	15.98	8.1	0.0394	1107.	25.41	0.292E-03	0.192E-05
208	0.0122		0.207	0.173	0.141	0.273E-05	0.980E-06	1.135	0.092	12.324	16.97	8.5	0.0415	1147.	24.12	0.689E-03	0.455E-05
209	0.0122	⊕	0.217	0.180	0.152	0.606E-05	0.989E-06	1.167	0.094	12.439	17.79	8.8	0.0430	1158.	23.24	0.151E-02	0.101E-04
210	0.0122		0.223	0.183	0.161	0.727E-05	0.972E-06	1.203	0.095	12.702	18.28	9.0	0.0438	1189.	22.81	0.180E-02	0.121E-04
211	0.0122		0.229	0.185	0.172	0.803E-05	0.957E-06	1.252	0.095	13.127	18.77	9.1	0.0444	1216.	22.50	0.196E-02	0.134E-04
212	0.0122	0.0050	0.238	0.191	0.184	0.133E-04	0.940E-06	1.289	0.097	13.324	19.51	9.4	0.0457	1255.	21.88	0.322E-02	0.222E-04
213	0.0122	0.0050	0.242	0.192	0.191	0.157E-04	0.995E-06	1.315	0.097	13.560	19.84	9.4	0.0460	1189.	21.75	0.376E-02	0.262E-04
214	0.0122	0.0050	0.251	0.198	0.200	0.194E-04	0.983E-06	1.328	0.099	13.464	20.57	9.7	0.0475	1224.	21.04	0.463E-02	0.323E-04
215	0.0122	0.0050	0.255	0.201	0.205	0.253E-04	0.100E-05	1.340	0.099	13.509	20.90	9.8	0.0481	1210.	20.80	0.601E-02	0.422E-04
216	0.0122	0.0050	0.189	0.162	0.120	0.875E-06	0.851E-06	1.058	0.089	11.883	15.49	7.9	0.0387	1277.	25.81	0.226E-03	0.146E-05
217	0.0122	0.0050	0.211	0.178	0.141	0.348E-05	0.851E-06	1.114	0.093	11.916	17.30	8.7	0.0427	1340.	23.43	0.887E-03	0.580E-05
218	0.0122	0.0050	0.230	0.192	0.160	0.634E-05	0.851E-06	1.159	0.097	11.958	18.85	9.4	0.0459	1390.	21.77	0.160E-02	0.106E-04
219	0.0122	0.0050	0.245	0.201	0.180	0.121E-04	0.851E-06	1.224	0.099	12.342	20.08	9.8	0.0481	1422.	20.79	0.299E-02	0.202E-04
301	0.0122	0.0150	0.070	0.066	0.041	0.250E-05	0.112E-05	0.976	0.099	9.885	5.74	9.8	0.0477	1081.	20.98	0.715E-03	0.417E-05
302	0.0122	0.0150	0.080	0.075	0.050	0.117E-04	0.109E-05	1.042	0.105	9.894	6.56	11.1	0.0542	1176.	18.46	0.333E-02	0.195E-04
303	0.0122	0.0150	0.090	0.084	0.060	0.258E-04	0.108E-05	1.111	0.111	9.981	7.38	12.4	0.0605	1263.	16.52	0.729E-02	0.430E-04
304	0.0122		0.072	0.068	0.040	0.237E-05	0.107E-05	0.926	0.100	9.223	5.90	10.1	0.0492	1148.	20.31	0.681E-03	0.395E-05
305	0.0122	⊛	0.099	0.092	0.068	0.453E-04	0.110E-05	1.145	0.117	9.822	8.11	13.6	0.0664	1295.	15.07	0.128E-01	0.755E-04
306	0.0122		0.111	0.103	0.080	0.584E-04	0.109E-05	1.201	0.123	9.758	9.10	15.2	0.0740	1383.	13.51	0.164E-01	0.973E-04
307	0.0122		0.120	0.110	0.092	0.901E-04	0.111E-05	1.278	0.127	10.025	9.84	16.2	0.0794	1402.	12.60	0.250E-01	0.150E-03
308	0.0122	0.0150	0.114	0.105	0.086	0.690E-04	0.120E-05	1.257	0.124	10.114	9.34	15.5	0.0755	1259.	13.24	0.192E-01	0.115E-03
309	0.0122	0.0150	0.124	0.114	0.098	0.105E-03	0.116E-05	1.317	0.129	10.189	10.16	16.7	0.0817	1356.	12.24	0.290E-01	0.175E-03
310	0.0122	0.0150	0.095	0.089	0.064	0.287E-04	0.115E-05	1.123	0.114	9.827	7.79	13.1	0.0638	1217.	15.68	0.809E-02	0.478E-04
401	0.0122	0.0100	0.077	0.073	0.039	0.000E+00	0.955E-06	0.844	0.084	10.010	6.31	7.1	0.0348	1077.	28.77	0.000E+00	0.000E+00
402	0.0122	0.0100	0.089	0.083	0.048	0.000E+00	0.932E-06	0.899	0.090	9.944	7.30	8.2	0.0399	1183.	25.05	0.000E+00	0.000E+00
403	0.0122	0.0100	0.100	0.093	0.059	0.000E+00	0.915E-06	0.983	0.095	10.312	8.20	9.1	0.0444	1271.	22.51	0.000E+00	0.000E+00
404	0.0122	0.0100	0.111	0.102	0.069	0.302E-05	0.911E-06	1.036	0.100	10.345	9.10	10.0	0.0490	1341.	20.40	0.840E-03	0.503E-05
405	0.0122	0.0100	0.112	0.103	0.071	0.355E-05	0.911E-06	1.057	0.100	10.518	9.18	10.1	0.0493	1345.	20.28	0.985E-03	0.592E-05
406	0.0122		0.124	0.113	0.081	0.819E-05	0.905E-06	1.089	0.105	10.323	10.16	11.1	0.0544	1416.	18.40	0.226E-02	0.136E-04
407	0.0122	◇	0.136	0.124	0.093	0.132E-04	0.893E-06	1.140	0.110	10.349	11.15	12.1	0.0593	1504.	16.88	0.362E-02	0.220E-04
408	0.0122		0.142	0.128	0.102	0.191E-04	0.897E-06	1.197	0.112	10.680	11.64	12.6	0.0614	1525.	16.29	0.520E-02	0.318E-04
409	0.0122		0.151	0.135	0.111	0.290E-04	0.988E-06	1.225	0.115	10.630	12.38	13.3	0.0649	1423.	15.41	0.785E-02	0.481E-04
410	0.0122	0.0100	0.160	0.143	0.121	0.379E-04	0.969E-06	1.260	0.118	10.652	13.11	14.0	0.0684	1490.	14.62	0.102E-01	0.632E-04
411	0.0122	0.0100	0.170	0.151	0.133	0.466E-04	0.962E-06	1.304	0.122	10.723	13.93	14.8	0.0722	1542.	13.84	0.125E-01	0.777E-04
412	0.0122	0.0100	0.179	0.157	0.147	0.672E-04	0.939E-06	1.369	0.124	11.017	14.67	15.4	0.0754	1614.	13.26	0.178E-01	0.112E-03
413	0.0122	0.0100	0.119	0.109	0.075	0.571E-05	0.921E-06	1.050	0.104	10.142	9.75	10.7	0.0524	1372.	19.08	0.158E-02	0.952E-05
414	0.0122	0.0100	0.192	0.168	0.163	0.820E-04	0.932E-06	1.415	0.128	11.038	15.74	16.4	0.0803	1678.	12.45	0.216E-01	0.137E-03
415	0.0122	0.0100	0.104	0.097	0.058	0.625E-06	0.890E-06	0.929	0.098	9.526	8.52	9.5	0.0465	1338.	21.50	0.176E-03	0.104E-05
501	0.0122	0.0090	0.105	0.097	0.059	0.209E-06	0.930E-06	0.937	0.093	10.111	8.61	8.6	0.0419	1215.	23.85	0.584E-04	0.348E-06
502	0.0122	0.0090	0.115	0.106	0.068	0.961E-06	0.930E-06	0.986	0.097	10.198	9.43	9.3	0.0456	1268.	21.91	0.267E-03	0.160E-05
503	0.0122		0.125	0.114	0.080	0.385E-05	0.930E-06	1.067	0.100	10.648	10.25	10.0	0.0490	1314.	20.39	0.106E-02	0.642E-05
504	0.0122	⟐	0.143	0.129	0.097	0.120E-04	0.930E-06	1.131	0.107	10.599	11.72	11.4	0.0556	1399.	17.99	0.327E-02	0.200E-04
505	0.0122		0.152	0.136	0.108	0.196E-04	0.922E-06	1.184	0.110	10.811	12.46	12.0	0.0586	1449.	17.06	0.529E-02	0.327E-04
506	0.0122		0.161	0.143	0.118	0.280E-04	0.920E-06	1.222	0.112	10.868	13.20	12.6	0.0617	1490.	16.20	0.751E-02	0.467E-04
507	0.0122	0.0090	0.170	0.151	0.127	0.340E-04	0.911E-06	1.245	0.115	10.798	13.93	13.3	0.0650	1544.	15.39	0.910E-02	0.567E-04
508	0.0122	0.0090	0.188	0.165	0.147	0.450E-04	0.905E-06	1.303	0.121	10.799	15.41	14.6	0.0712	1627.	14.05	0.119E-01	0.750E-04
509	0.0122	0.0090	0.199	0.173	0.163	0.607E-04	0.909E-06	1.365	0.123	11.054	16.31	15.3	0.0745	1658.	13.42	0.159E-01	0.101E-03
601	0.0122	0.0125	0.080	0.076	0.044	0.751E-06	0.872E-06	0.917	0.096	9.517	6.56	9.3	0.0453	1348.	22.06	0.214E-03	0.125E-05
602	0.0122	0.0125	0.082	0.077	0.049	0.955E-06	0.872E-06	0.996	0.097	10.251	6.72	9.4	0.0461	1359.	21.68	0.271E-03	0.159E-05
603	0.0122	0.0125	0.090	0.084	0.054	0.381E-05	0.866E-06	1.000	0.102	9.828	7.38	10.4	0.0506	1433.	19.77	0.108E-02	0.635E-05
604	0.0122	0.0125	0.093	0.087	0.059	0.531E-05	0.878E-06	1.057	0.103	10.252	7.62	10.6	0.0520	1433.	19.24	0.150E-02	0.885E-05
605	0.0122		0.099	0.092	0.064	0.926E-05	0.862E-06	1.077	0.106	10.135	8.11	11.3	0.0552	1505.	18.11	0.260E-02	0.154E-04
606	0.0122	⊛	0.104	0.097	0.069	0.141E-04	0.878E-06	1.106	0.109	10.164	8.52	11.8	0.0578	1512.	17.29	0.395E-02	0.235E-04
607	0.0122		0.109	0.101	0.074	0.201E-04	0.876E-06	1.131	0.111	10.173	8.93	12.4	0.0605	1549.	16.54	0.562E-02	0.335E-04
608	0.0122		0.113	0.104	0.078	0.288E-04	0.878E-06	1.150	0.113	10.170	9.26	12.8	0.0625	1572.	15.99	0.803E-02	0.480E-04
609	0.0122	0.0125	0.124	0.114	0.089	0.446E-04	0.876E-06	1.196	0.118	10.121	10.16	14.0	0.0683	1642.	14.65	0.124E-01	0.743E-04
610	0.0122	0.0125	0.127	0.116	0.094	0.453E-04	0.870E-06	1.234	0.119	10.333	10.41	14.3	0.0696	1674.	14.36	0.125E-01	0.755E-04
611	0.0122	0.0125	0.134	0.123	0.100	0.555E-04	0.868E-06	1.244	0.123	10.147	10.98	15.0	0.0734	1723.	13.62	0.153E-01	0.925E-04
612	0.0122	0.0125	0.151	0.137	0.119	0.866E-04	0.884E-06	1.313	0.130	10.140	12.38	16.8	0.0820	1788.	12.20	0.237E-01	0.144E-03

Table 2b Summary of data (steady, uniform flow); sediment II

No	d_{50} (m)	S_o	h (m)	R_h (m)	Q (m^3/s)	Qs_o (m^3/s)	ν (m^2/s)	U (m/s)	U* (m/s)	U/U*	h/d50	τ (N/m^2)	τ*	Re*	Ψ	Φ	qs_o (m^2/sm)
701	0.0235	0.0150	0.153	0.141	0.121	0.195E-05	0.886E-06	1.318	0.144	9.162	6.51	20.7	0.0516	3816.	19.38	0.201E-03	0.325E-05
702	0.0235	0.0150	0.161	0.147	0.131	0.293E-05	0.882E-06	1.356	0.147	9.207	6.85	21.7	0.0541	3924.	18.49	0.300E-03	0.488E-05
703	0.0235	0.0150	0.168	0.153	0.140	0.471E-05	0.874E-06	1.389	0.150	9.247	7.15	22.6	0.0562	4039.	17.78	0.481E-03	0.785E-05
704	0.0235	0.0150	0.182	0.166	0.152	0.107E-04	0.870E-06	1.392	0.156	8.905	7.74	24.4	0.0609	4222.	16.42	0.109E-02	0.178E-04
705	0.0235	0.0150	0.179	0.164	0.145	0.767E-05	0.867E-06	1.350	0.155	8.690	7.62	24.1	0.0602	4211.	16.62	0.787E-03	0.128E-04
706	0.0235		0.187	0.170	0.160	0.207E-04	0.904E-06	1.426	0.158	9.019	7.96	25.0	0.0623	4110.	16.05	0.211E-02	0.345E-04
707	0.0235		0.190	0.172	0.169	0.285E-04	0.890E-06	1.482	0.159	9.327	8.09	25.3	0.0630	4159.	15.88	0.288E-02	0.475E-04
708	0.0235	⊡	0.196	0.176	0.181	0.409E-04	0.911E-06	1.539	0.161	9.567	8.34	25.9	0.0645	4150.	15.50	0.411E-02	0.682E-04
709	0.0235		0.210	0.189	0.189	0.591E-04	0.917E-06	1.500	0.167	8.988	8.94	27.8	0.0694	4277.	14.40	0.596E-02	0.985E-04
710	0.0235	0.0150	0.187	0.171	0.155	0.147E-04	0.915E-06	1.381	0.159	8.716	7.96	25.1	0.0626	4071.	15.97	0.150E-02	0.245E-04
711	0.0235	0.0150	0.167	0.153	0.134	0.557E-05	0.906E-06	1.337	0.150	8.909	7.11	22.5	0.0562	3894.	17.60	0.572E-03	0.928E-05
712	0.0235	0.0150	0.159	0.146	0.124	0.182E-05	0.900E-06	1.300	0.147	8.856	6.77	21.5	0.0537	3832.	18.62	0.188E-03	0.303E-05
713	0.0235	0.0150	0.151	0.140	0.112	0.696E-06	0.886E-06	1.236	0.143	8.616	6.43	20.6	0.0513	3805.	19.49	0.722E-04	0.116E-05
801	0.0235	0.0200	0.125	0.118	0.088	0.134E-05	0.958E-06	1.173	0.152	7.702	5.32	23.2	0.0579	3737.	17.29	0.142E-03	0.223E-05
802	0.0235	0.0200	0.123	0.117	0.084	0.141E-05	0.943E-06	1.138	0.151	7.523	5.23	22.9	0.0571	3770.	17.52	0.150E-03	0.235E-05
803	0.0235		0.136	0.128	0.101	0.516E-05	0.949E-06	1.238	0.158	7.809	5.79	25.1	0.0626	3925.	15.97	0.544E-03	0.860E-05
804	0.0235	⊠	0.141	0.132	0.109	0.118E-04	0.947E-06	1.288	0.161	7.998	6.00	25.9	0.0647	3997.	15.46	0.124E-02	0.197E-04
805	0.0235		0.146	0.136	0.120	0.260E-04	0.945E-06	1.370	0.163	8.383	6.21	26.7	0.0666	4064.	15.02	0.271E-02	0.433E-04
806	0.0235		0.153	0.142	0.128	0.458E-04	0.943E-06	1.394	0.167	8.344	6.51	27.9	0.0696	4164.	14.37	0.477E-02	0.763E-04
807	0.0235	0.0200	0.168	0.156	0.139	0.772E-04	0.943E-06	1.379	0.175	7.870	7.15	30.7	0.0765	4366.	13.07	0.605E-02	0.129E-03
808	0.0235	0.0200	0.162	0.149	0.145	0.858E-04	0.943E-06	1.492	0.171	8.712	6.89	29.3	0.0731	4267.	13.68	0.886E-02	0.143E-03
901	0.0235	0.0250	0.094	0.090	0.059	0.255E-06	0.941E-06	1.046	0.149	7.023	4.00	22.2	0.0553	3712.	18.08	0.275E-04	0.425E-06
902	0.0235	0.0250	0.100	0.096	0.065	0.526E-06	0.939E-06	1.083	0.153	7.058	4.26	23.6	0.0587	3841.	17.03	0.566E-04	0.877E-06
903	0.0235	0.0250	0.104	0.100	0.070	0.272E-05	0.926E-06	1.122	0.156	7.174	4.43	24.4	0.0609	3960.	16.41	0.292E-03	0.453E-05
904	0.0235		0.109	0.104	0.074	0.751E-05	0.918E-06	1.131	0.160	7.070	4.64	25.6	0.0638	4097.	15.66	0.606E-03	0.125E-04
905	0.0235	⊞	0.112	0.107	0.079	0.112E-04	0.908E-06	1.176	0.162	7.257	4.77	26.2	0.0654	4193.	15.29	0.120E-02	0.187E-04
906	0.0235		0.114	0.108	0.085	0.172E-04	0.932E-06	1.243	0.163	7.619	4.85	26.6	0.0663	4112.	15.08	0.183E-02	0.287E-04
907	0.0235		0.122	0.116	0.091	0.383E-04	0.929E-06	1.243	0.169	7.368	5.19	28.5	0.0710	4268.	14.09	0.408E-02	0.638E-04
908	0.0235	0.0250	0.119	0.113	0.095	0.486E-04	0.929E-06	1.331	0.166	8.007	5.06	27.6	0.0688	4204.	14.53	0.515E-02	0.810E-04
909	0.0235	0.0250	0.129	0.121	0.110	0.113E-03	0.925E-06	1.421	0.173	8.238	5.49	29.8	0.0742	4383.	13.48	0.119E-01	0.188E-03

LEGEND:

No : running number of experiment
d_{50} : sediment I and II
S_o : slope (indicated are also the symbols used in the figures)
h : water depth
R_h : hydraulic radius
Q : water discharge, measured with flowmeter
Qs_o : sediment discharge (volume of particles only), measured with sediment-measuring device
ν : viscosity, measured through water temperature
U : average flow velocity, calculated by $U = Q/hb$
U* : friction velocity, calculated by $U_* = \sqrt{gR_hS_o}$
U/U*: dimensionless velocity, calculated
h/d_{50}: relative depth, calculated
τ : bottom shear stress, calculated by $\tau = \rho U_*^2$
τ* : dimensionless shear stress, calculated by $\tau_* = \tau/gd_{50}(\rho_s - \rho)$
Re* : particle Reynolds number, calculated by $Re_* = U_* d_{50}/\nu$
Ψ : shear intensity parameter, calculated by $\Psi = 1/\tau_*$
Φ : sediment transport parameter, calculated by $\Phi = Qs_o R_h U/Q\sqrt{gd_{50}^3(\rho_s/\rho - 1)}$
qs_o : unit sediment discharge, calculated by $qs = Qs_o/b$, where b = 0.6 m

$$\Psi = g(\rho_s-\rho)d_{50}/(\gamma R_h S_0)$$

was related to the sediment-transport parameters,

$$\Phi = CUR_h/\sqrt{(\rho_s/\rho - 1)\ gd_{50}^3}$$

with C as the volumetric concentration of the transported particles and given as $C = Qs_0/Q$. A relationship was established by Graf and Acaroglu (1968) for flume and river data (as well as closed conduit data) such as:

$$\Phi = 10.4\ \Psi^{-2.5} \qquad (1)$$

it is reproduced here with fig. 5; having its validity between $10^{-2} < \Phi < 10^3$. Earlier Graf, Cao and Suszka (1983) showed that the relationship of eq. (1) is not valid for $\Phi < 10^{-2}$, but arrives at extremely low Φ - values at Ψ = 15 (see Graf, Cao and Suszka (1983, fig. 3)). The data used to obtain the above conclu-

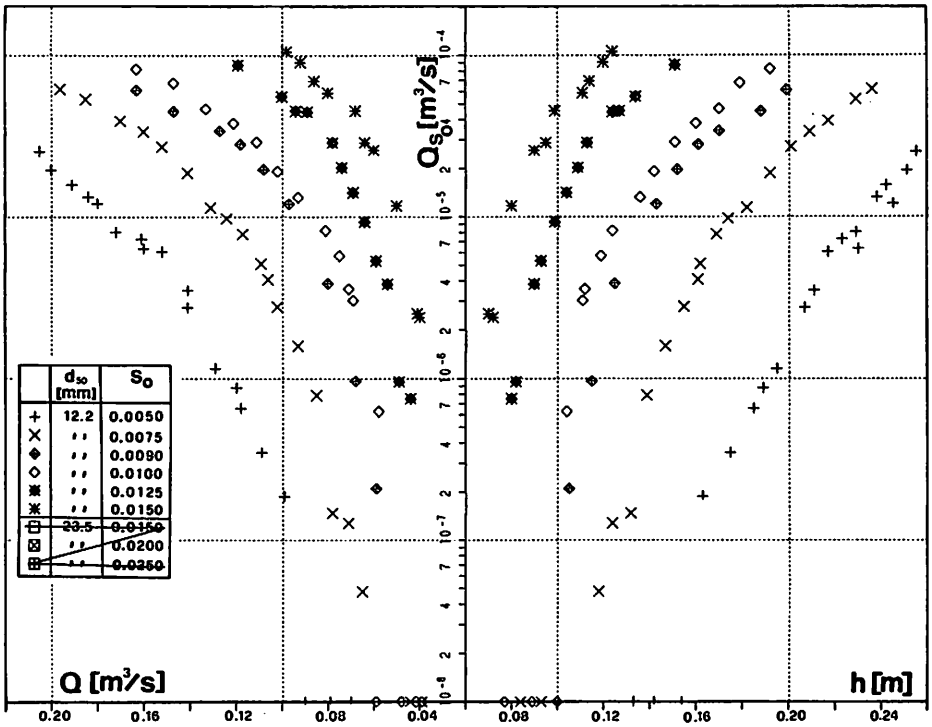

Fig. 3a Sediment discharge, Qs_0, versus water depth, h, and water discharge, Q, for present experiments (see Table 2a); sediment I

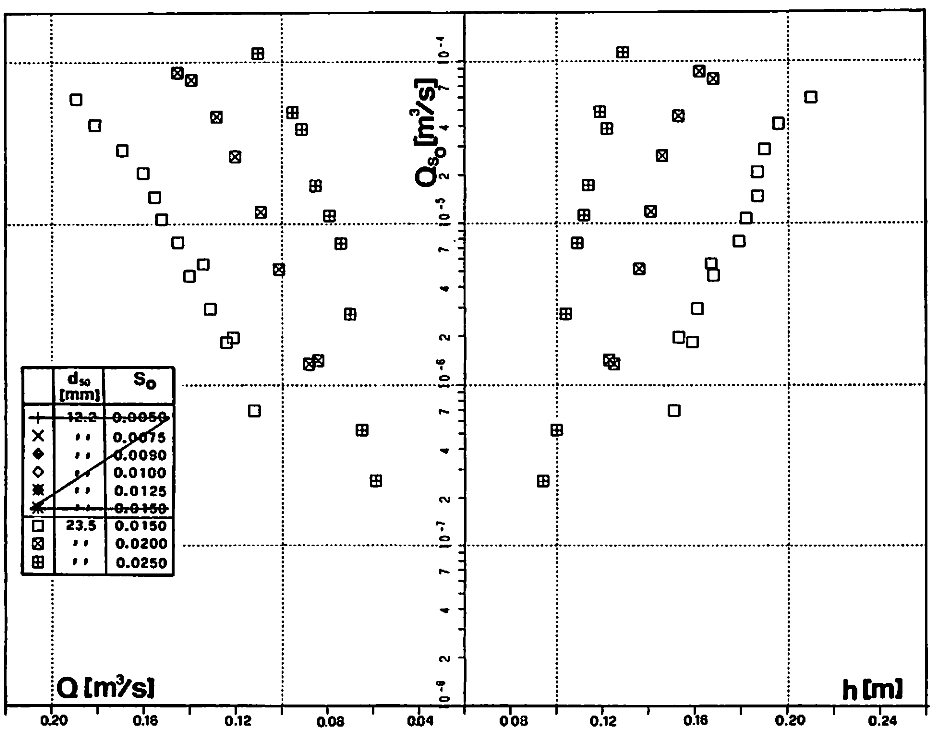

Fig. 3b Sediment discharge, Qs_0, versus water depth, h, and water discharge, Q, for present experiments (see Table 2b); sediment II

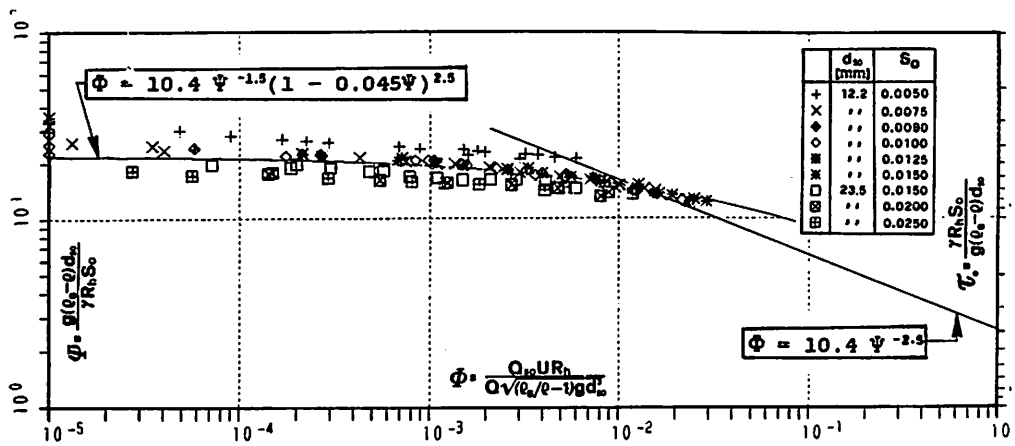

Fig. 4 Shear-intensity parameter, Ψ, versus sediment-transport parameter, Φ; shown are the data given in Tables 2a and b. Eq. (2) is fitted through the data, it is valid for $\Psi > 14.6$; eq. (1) takes over for $\Psi < 14.6$

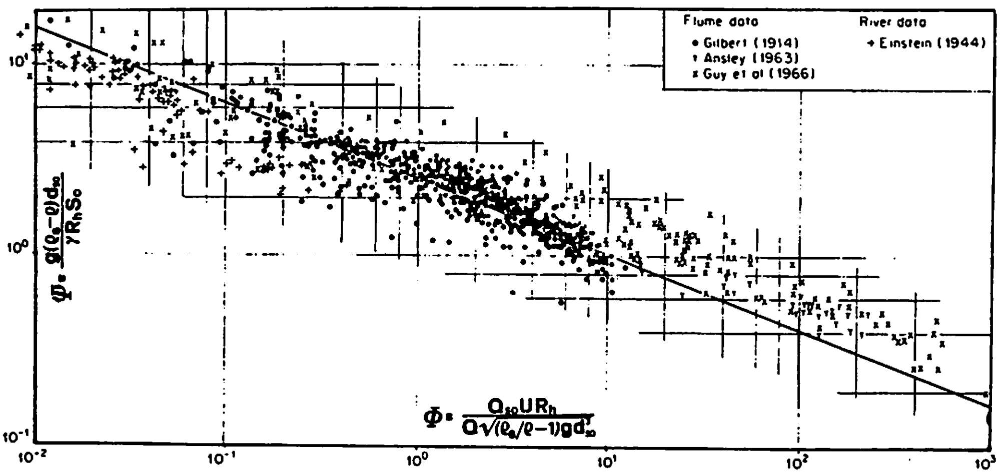

Fig. 5 Shear-intensity parameter, Ψ, versus sediment-transport parameter, Φ, shown are the data of Gilbert, Ansley, Guy et al. and Einstein (from Graf (1971, p. 220)). Eq. (1) is fitted through the data

sions have been extended since and are now presented in fig. 4. Note in the legend of fig. 4 that for the two sediments investigated, the slope variation was considerable; in general these slopes may be considered as "steep" ones. A good fit for present data was obtained by:

$$\Phi = 10.4\ \Psi^{-1.5}(1 - 0.045\ \Psi)^{2.5} \qquad (2)$$

where the constant of 0.045^{-1} represents in a way a limiting (or critical) Ψ - value or $\Psi^{-1} = 0.045$. The relation of eq. (2) is thus valid for $\Phi < 10^{-2}$ or $\Psi > 14.6$ and merges beyond these values with the relation of eq. (1). Thus for a large range of Φ - values i.e.: $10^{-5} < \Phi < 10^3$ a relationship is found such as:

$$\Phi = K(10.4\ \Psi^{-1.5}) \text{ with } \begin{array}{ll} K = \Psi^{-1} & \text{for } \Psi < 14.6 \\ K = (1 - 0.045\ \Psi)^{2.5} & \text{for } \Psi > 14.6 \end{array} \qquad (3)$$

Two independent data sets, one obtained by Cao (1985) - using the same installation, but measuring the sediment discharge differently - and one by

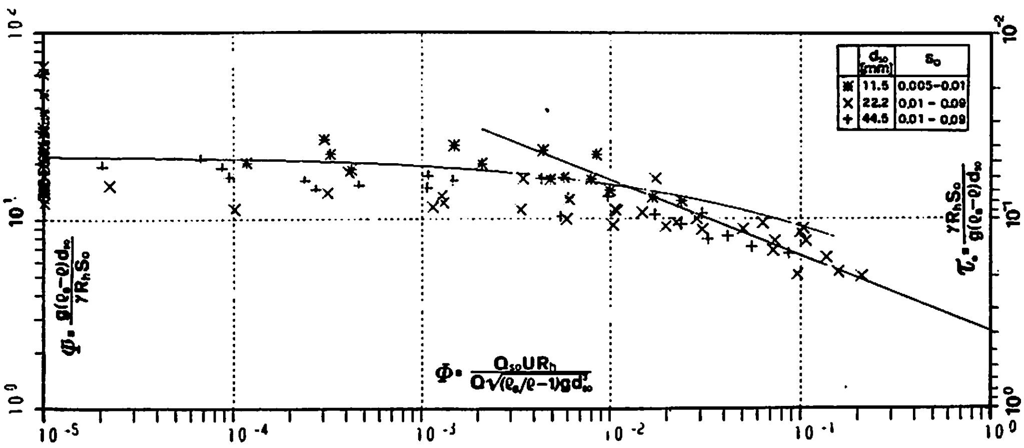

Fig. 6 Shear-intensity parameter, Ψ, versus sediment-transport parameter, Φ, shown are the data of Cao (1985) with the relation given by eq. (1) and eq. (2)

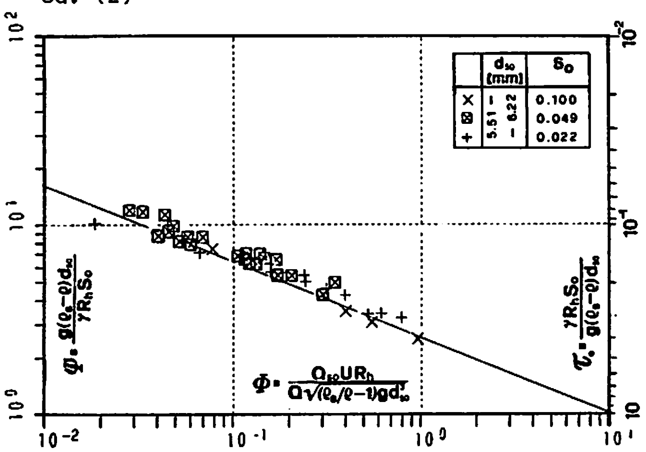

Fig. 7 Shear-intensity parameter, Ψ, versus sediment-transport parameter, Φ, shown are the data of Mizuyama (1977) with the relation given by eq. (1)

Mizuyama (1977) are available to test the generality of the relation of eq. (3). These data, when represented on the Φ vs. Ψ plot on figs. 6 and 7, show the same tendency as expressed by the relations of eq. (3). Furthermore, it should be noted, that a similar relationship was proposed by Chang (1980) as well as Parker (1979).

In summary, it is concluded that the relations of eq. (3) explain the present data, as well as the ones of Cao (1985) and of Mizuyama (1977, p. 93), sufficiently well. Nevertheless, close observation of the data in figs. 4, 6 and 7 shows that the scatter in the lower sediment-transport ranges, is somehow systematic with respect to the slope, S_0, and lesser so with respect to the sediment size, d_{50}. This raises the question, whether the limiting Ψ - values depend upon the slope, S_0, sediment size, d_{50}, or a combination of both.

Begin of sediment transport: It is rather subjective (due to different definitions and measuring methods!) to define the beginning of sediment transport. Nevertheless such a definition has a favorable response, notably through presentation in form of a dimensionless shear stress, $\tau = \Psi^{-1}$. Shields (1936) proposed a relationship which is given with fig. 8, of dimensionless shear-stress, τ^*, versus particle Reynolds number, U^*d_{50}/ν. Note that both, the slope, S_0, via $U^* = \sqrt{gR_hS_0}$, and the particle sediment size, d_{50}, enter these

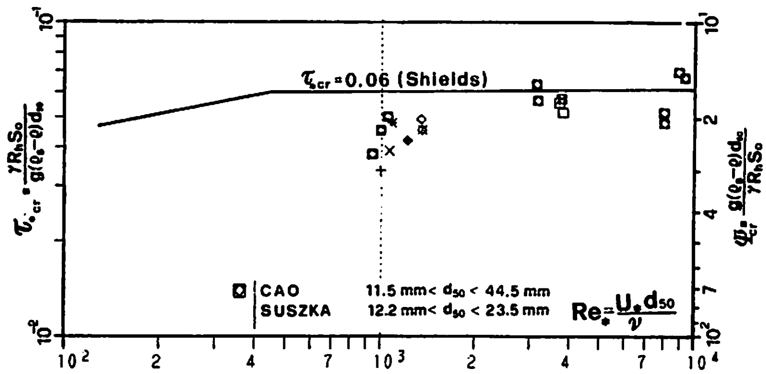

Fig. 8 Dimensionless critical shear stress, τ^*_{cr}, and critical shear-intensity parameter, Ψ_{cr}, vs. particle Reynolds number, Re*; shown are the present data (see Tables 2a and b) and the data of Cao (1985)

parameters. On fig. 8 are plotted the present data as well as the ones of Cao (1985) and are compared with the Shields' critical value extrapolated as being τ^*_{cr} = 0.06 and constant within the range of Re* > $4 \cdot 10^2$ (see Graf (1971, p. 97)). These data sets indicate, that a constant critical shear stress is not warranted. While these data are insufficient to draw a conclusion, it can be observed that the larger the Re* values, the larger will be the τ^*_{cr} values.

Yet another way of looking at the present data, augmented by the ones of Cao (1985) and of Mizuyama (1977, p. 60), is done in fig. 9, where the dimensionless critical shear-stress, τ^*_{cr}, is plotted against the slope, S_0. Here it becomes rather evident that for Re* > $5 \cdot 10^2$ the dimensionless critical shear-stress, τ^*_{cr}, is dependent on the slope, S_0. Fitting a relation to the data, one obtains:

$$\tau^*_{cr} = 0.042 \cdot 10^{2 \cdot 2 S_0} \tag{4}$$

The dependency of the critical dimensionless shear stress, τ^*_{cr}, on the slope, S_0, already indicated by Mizuyama (1977, p. 92) is thus further evidenced. Note that the average value for the region of the present experimental data i.e.: for $0.005 < S_0 < 0.025$ is given by τ^*_{cr} = 0.045, the very value used in eq. (2).

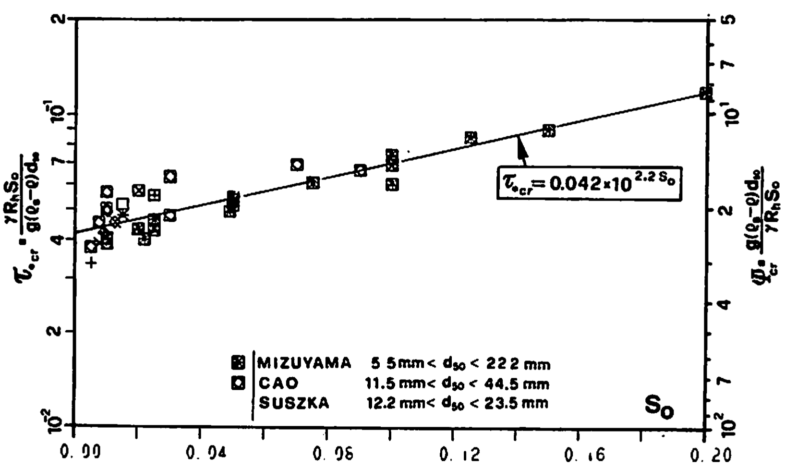

Fig. 9 Dimensionless critical shear stress, τ^*_{cr}, and critical shear-intensity parameter, Ψ_{cr}, vs. bed slope of the flume, S_0; shown are the present data and the data of Cao (1985) and of Mizuyama (1977)

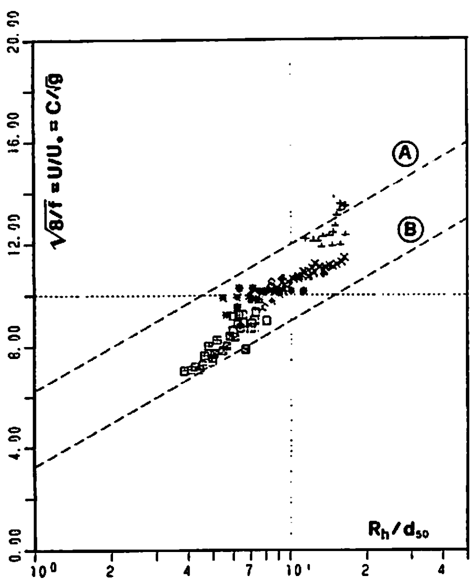

Fig. 10 Flow-resistance relation: $\sqrt{8/f}$ versus R_h/d_{50}; present data are compared with
A. relation of Keulegan (£ = 6.25) and
B. relation of Graf, Cao and Suszka (£ = 3.25); the range of Ψ values is found in Table 2

Flow resistance: For steady, uniform flows the flow resistance is commonly expressed by Weisbach-Darcy relationship (Graf (1971, 11.2)) which gives the friction slope, S, as

$$S = f\ (1/4R_h)\cdot(U^2/2g) \qquad (5)$$

where R_h is the hydraulic radius; f is the friction factor which can be given as

$$\sqrt{8/f} = U/U^* = C/\sqrt{g} \qquad (6)$$

where C is the Chézy friction factor; U* is the bed-shear velocity; and U/U* represents the velocity distribution. Generally the friction factor depends on the flow Reynolds and Froude numbers, Re and Fr; the relative water depth, R_h/k_s; the flow sinuosity, ξ; and the shear intensity, Ψ; where k_s is the equivalent sand roughness of the bed material. For hydraulically rough flow in steep channels being reasonably straight, it was shown by Graf (1984) that both, flow Reynolds and Froude numbers are not important parameters, so that

$$\sqrt{8/f} = fn(R_h/k_s,\ \Psi) \qquad (7)$$

It seems reasonable, at least as a first attempt, to assume that the relative depth, R_h/k_s, is the most important of the parameters in the function, fn. Data available from an earlier study at the LHYDREP were plotted according to the relation of eq. (7) by Graf, Cao and Suszka (1983) and the following relation was obtained

$$\sqrt{8/f} = 5.75\ \log(R_h/k_s) + £ \qquad (8)$$

by eye-fitting with $£_{50} = 3.25$ at $k_s = d_{50}$ or $£_{84} = 4.0$ at $k_s = d_{84}$. Subsequently Graf (1984) and Cao (1985) have found that above relation explains their data reasonably well. The present data, presented herewith in fig. 10, are in overall agreement with this conclusion.

CONCLUSIONS

Sediment transport, mainly as bed load, is experimentally investigated. An existing laboratory facility (fig. 1) was modified in a way that the determination of the sediment transport is continuous and very accurate. The most important single item was the development of a sediment-measuring device (fig. 2).

The data are presented in the form of tables (tables 2a and b) and graphically (fig. 3a and b). These data supplement well the already existing data sets, since they are derived with relatively steep channel slopes ($0.005 < S_0 < 0.025$). It is believed that the present data set is of high precision, as far as the sediment-discharge measurements are concerned.

The present data, together with data sets available in the literature, are also presented in dimensionless form. A resulting relation, given with eq. 3, explains reasonably well the sediment transport; it can be seen in figs. 4, 5, 6 and 7.

Furthermore, the present investigation proposes a relation, given with eq. 4 and fig. 9, for determination of the begin of sediment transport, and this for slopes of $S_0 < 0.20$. To be noted is, that the well-known Shields criteria is insufficient for such large slopes.

A flow-resistance relation, proposed earlier by Graf (1984) for steep channels with small relative depth, R_h/k_s, was found to be justified. To be noted is, that this proposed relation, given with eq. 8, is different from the well-known Keulegan relation.

The results of the present investigation should be particularly useful for engineers designing channels or gullies in mountaineous regions, where large slopes and small relative depths are frequently encountered.

REFERENCES

Cao, H.H. (1985): "Resistance hydraulique d'un lit de gravier mobile à pente raide, étude expérimentale"; doctoral dissertation, Ecole Polytechnique Fédérale, Lausanne, Suisse.

Chang, H.H. (1980): "Geometry of Gravel Streams"; Proc., Am. Soc. Civ. Engs., Vol. 106, HYO.

Graf, W.H. (1984): "Hydraulics of Sediment Transport"; Water Res. Publ., Littleton, Colorado (formely McGraw-Hill Inc., 1971).

Graf, W.H. (1984); "Flow Resistance for Steep, Mobile Channels"; Seminar "Idraulica de Territorio Montano", Bressanone, Univ. Padua, Italy, Oct.

Graf, W.H., Cao, H.H. and Suszka, L. (1983); "Hydraulics of Steep, Mobile-Bed Channels"; Proc., XX Congress, Int. Ass. Hydr. Res., Vol. 7; Moscow, USSR.

Graf, W.H. and Suszka, L. (1985); "Unsteady Flow and its Effedt on Sediment Transport", Proc., XXI Congress, Int. Ass. Hydr. Res., Vol. 3; Melbourne, Australia.

Mizuyama, T. (1977): "Bed Load Transport in Steep Channels"; doctoral dissertation, Kyoto Univ., Kyoto, Japan.

Parker, G. (1979): "Hydraulic Geometry of Active Gravel Rivers"; Proc., Am. Soc. Civ. Engs., Vol. 105, HY9.

Suszka, L. (1986); "Sediment Transport in Steep Channels, a Laboratory Investigation"; draft for a doctoral dissertation, Ecole Polytechnique Fédérale, Lausanne, Suisse.

APPENDIX - NOTATION

The following symbols are used in this paper:

C	= volumetric concentration, given as $C = Q_{s0}/Q$;
d_{50}	= diameter of sediment;
h	= water depth;
h/d_{50}	= relative depth, calculated;
R_h	= hydraulic radius;
Re^*	= particle Reynolds number, calculated by $Re^* = U \cdot d_{50}/\nu$;
S_0	= slope;
Q	= water discharge, measured with flowmeter;
qs_0	= unit sediment discharge, calculated by $qs = Qs_0/b$, where b = 0.6 m;sediment discharge (volume of particles only),
Qs_0	= measured with sediment-measuring device;
U	= average flow velocity, calculated by $U = Q/hb$;
U^*	= friction velocity, calculated by $U_0 = \sqrt{gR_hS_0}$;
U/U^*	= dimensionless velocity, calculated;
ν	= viscosity, measured through water temperature;
τ	= bottom shear stress, calculated by $\tau = \rho U^{*2}$;
τ^*	= dimensionless shear stress, calculted by $\tau^* = \tau/gd_{50}(\rho_0-\rho)$;
ψ	= shear intensity parameter;
Φ	= sediment transport parameter.